International Journal of Scientific Reports
Dutta K et al. Int J Sci Rep. 2024 Jul;10(7):225-233
http://www.sci-rep.com

pISSN 2454-2156 | eISSN 2454-2164

DOI: https://dx.doi.org/10.18203/issn.2454-2156.IntJSciRep20241592

Original Research Article

Explanation based on thermodynamic parameters regarding effect of sensing film thickness and amount of graphene oxide on sensor performance in aniline, N-phenylglycine and graphene oxide based electrochemical heavy metal ion sensor

Kusumita Dutta*, Siddhartha Panda

Department of Chemical Engineering, National Centre for Flexible Electronics, Indian Institute of Technology Kanpur, Kanpur, UP, India

Received: 15 May 2024
Revised: 21 May 2024
Accepted: 28 May 2024

***Correspondence:**
Dr. Kusumita Dutta,
E-mail: kusumitasword@gmail.com

ABSTRACT

Background: To construct a heavy metal ion sensor, selectivity and sensitivity are the key important parameters to be taken care of. In our earlier work, film thickness and amount of graphene oxide (GO) content in a novel composite ANGO, synthesized from aniline, N-phenylglycine and GO was varied and sensing parameters including sensitivity, limit of detection (LOD), thermodynamic parameter which includes $-\Delta G_{ad}$ and charge transport parameter including barrier width (BW), d, of charge transfer based on Simmon's model were evaluated and compared and an LOD of 800 ppt for Cd^{2+} was achieved using square wave voltammetry (SWV) withstanding interference from several ions.
Methods: In this work, thermodynamic factors such as $-\Delta G_{ad}$, ΔH, reorganization energy, partition coefficient and solvated ionic radius were used to explain the sensor performance with respect to film thickness and amount of GO. All the parameters were analyzed for different film thicknesses and amount of GO and a correlation was achieved. Finally, effect of electrochemical surface area of different polyaniline-based material on thermodynamic properties of detection process of Cd^{2+} was studied.
Results: The variation of the thermodynamic properties for Cd^{2+} sensing with respect to film thickness and amount of GO were examined. Similarly, variation of thermodynamic properties for polyaniline based different sensing materials were examined. Correlation coefficients were developed from the thermodynamic parameters and the d values to explain the underlying mechanism behind improved sensor performance.
Conclusions: This study can provide information on the thermodynamic properties which can be predicted from BW technique. The correlation coefficients would help in designing polyaniline based novel sensing film material with the need of lesser number of experiments.

Keywords: Heavy metal, Partition coefficient, Enthalpy, Reorganization energy, Square wave voltammetry, Barrier width, Solvated ionic radius

INTRODUCTION

For an electrochemical sensor, selectivity and sensitivity are the important performance parameter.[1,2] For the efficient charge transport the film thickness as well as the sensing material play a crucial role. It is reported that the thickness of the sensitive layer has great influence on sensor performance.[3] In an earlier work, we have demonstrated how the sensor activity in an electrochemical sensor for detection of Cd^{2+} depends on the electrode thickness as well as incorporation of amount of graphene oxide (GO) in the sensing film using a novel sensing material, named ANGO synthesized from aniline, N-phenylglycine and GO.[4] To understand the mechanism

for the improved sensor performance, thermodynamic analysis based on chemisorption and charge transport analysis based on the barrier with (BW) technique were conducted with different film thicknesses and varying concentration of sensing material. The BW technique based on Simmon's model incorporating tunneling mechanism was used in variety of other electrochemical works.[5-11] Both the results obtained from the thermodynamic and charge transport analysis were complementary to each other. Further reduction in film thickness, the sensor performance was improved to obtain a LOD of 800 ppt of Cd^{2+}. The detection process of Cd^{2+} is illustrated in Figure 1. Briefly, the sensing material ANGO (1-9) of varying thicknesses with varying amount of GO were electrodeposited on stainless steel electrode and functionalized with iminodiacetate (IDA) group.[4] The IDA functionalized electrodes were immersed in Cd^{2+} containing solution for 30 min without applying any external potential. Next, -1.2 V was applied and the ions get deposited onto the surface, following to this, the ions gets stripped out from the film at -0.78 V, giving rise a square wave voltammetry (SWV) peak for Cd^{2+} when the voltage was varied from -1.2 V to 0.05 V using a SW pulse.

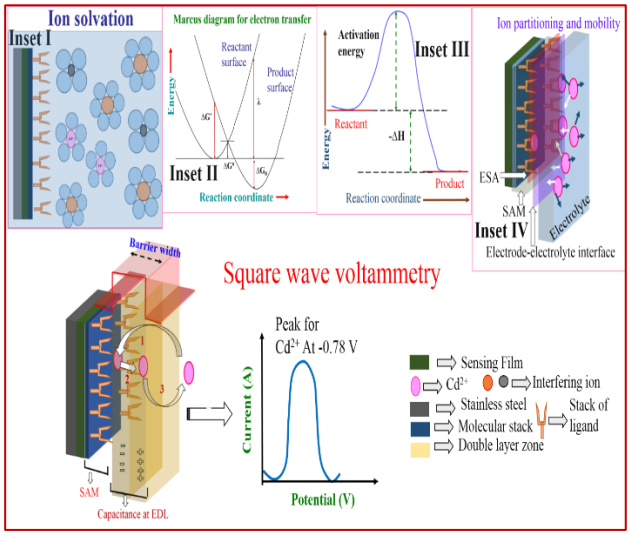

Figure 1: Schematic of the detection process of Cd^{2+} by SWV with possible mechanisms of charge transport. Inset I: ion solvation; inset II: Marcus diagram for electron transfer; inset III: Enthalpy and activation energy to explain the reaction mechanism; inset IV: Partitioning of ion between the electrode and electrolyte at the electrode electrolyte interface.[12]

Surface functionalization with iminodiacetate group provides a self-assembled monolayer (SAM) at the electrode surface. At -1.2 V, it can be expected that Cd^{2+} ions get diffused across the double layer zone to the surface and adsorbed into the nearby active sites available. There are several reports where the SAM modified electrodes were found to be useful in studying long range electron transfer between the electrodes and redox active species.[13-17]As described by Marcus, the electron transfer rate constant depends on the free energy barrier which in turn depends on the reorganization energy (λ).[18,19] λ can be defined as the energy required for distorting the nuclear configuration from the donor state to the acceptor state without any electron transfer. It may be understood by considering a model in which rapid electron transfer from reactant to the product is accompanied with no relaxation of the nuclear configuration in the reactants following relaxation of the nuclear configuration of the product where the free energy change is equal to (-λ).[12] Figure 1, inset I and II, shows the ion solvation and Marcus's diagram of electron transfer respectively.

The Cd^{2+} detection process by SWV involves adsorption of Cd^{2+} at -1.2 V and desorption process at 0.78 V. This adsorption of Cd^{2+} ions from electrolyte to the electrode surface is accompanied by partitioning of ions among the electrode surface and the electrolyte which can be measured as partition coefficient. It can be defined the ratio of concentration of ions in one medium to that in the other medium at equilibrium.[20] A pictorial representation of ion partitioning between the electrode surface and electrolyte is portrayed in inset IV, in Figure 1. $-\Delta G_{ad}$ values, as mentioned in our earlier work, was found to be increasing with increase in amount of GO and decrease in film thickness, therefore, it can be understood that ion partitioning can significantly get affected by the film thickness and amount of GO content. Thus, it can explain the reason behind improvement in sensor performance. Partition coefficient is used widely to explain the transport mechanism for several pollutants, drugs etc.[21]

Similarly, it can be expected that due to change in $-\Delta G_{ad}$ values, corresponding change in ΔH can be expected which in turn can explain the improvement in sensor performance due to lowering the film thickness and increase in GO content. As shown in inset III of Figure 1, to bring about a reaction successfully, activation energy is required. Total energy requiring the reaction includes enthalpy ΔH. In absence of any barrier, the energy required will be lower as compared to that in presence of any barrier. Higher film thickness and lower amount of GO can be explained as barrier as it deteriorated sensor performance. Therefore, lower lower film thickness and higher amount of GO catalyzes sensing process. In presence of catalysts, total energy requirement is lower than that in absence of catalysts.[22] To support the fact it is important to evaluate ΔH for each case.

From the above explanations it can be understood that the thermodynamic properties-enthalpy, reorganization energy, partition coefficient can be used to explain sensor performance with different film thicknesses and amount of GO. A similar study was conducted in our earlier work for polyaniline and N-phenylglycine based sensor to understand the influence of interferants on the thermodynamic properties.[23] This work is a follow up work of our previous work.[4] These factors were used to explain the charge transport mechanism behind the

detection of Cd^{2+} and compared with BW technique as performed in our previous work.[4] Finally, the thermodynamic factors, partition coefficient and BW (d) values were fitted to obtain a inter-relation which in turn can explain the mechanism of charge transfer.

METHODS

1-ethyl-3-(3-dimethylaminopropyl) carbodiimide hydrochloride (EDC), N-phenylglycine and N-hydroxysuccinimide (NHS) were obtained from Sigma Aldrich (USA) graphite flakes and cadmium chloride, were purchased from Rankem (India); sulfuric acid ($H_2SO_4.6H_2O$) and triethylamine were purchased from Qualigens (USA); di-sodium hydrogen phosphate, hydrochloric acid and diethylamine were purchased from Merck (Germany); aniline were procured from Loba Chemicals (Mumbai, India).

The solutions were made with double distilled water (conductivity ≤0.2 µS/cm). Electrochemical tests were carried out using Auto-lab PGSTAT 302N (Eco Chemie, The Netherlands). For counter electrode and reference electrode, platinum rod and saturated Ag/AgCl were used respectively. An 1 mm thick stainless steel (SS, 304) plate with area of (1.5×1) cm served as the working electrode onto which the composite was deposited. A glass cell having working volume of 50 ml was fitted so that the reference electrode was fixed closer to the working electrode than the counter electrode. For electrochemical synthesis of the ANGO composite, the electrode was dipped into the electrolyte at a depth of 0.5 cm so that the effective geometrical surface area equal of 1.5 cm^2 (i.e., both surfaces of (0.5×1.5) cm) was maintained for metal ion sensing.

Experimental methods

The study period for design, experiments, analysis, simulation and interpretation for this work was from April 2020 to November 2023. The experiments were conducted in department of chemical engineering, Indian Institute of technology Kanpur.

The experimental condition and methods were the same as mentioned in our previous work.[24] Therefore, not described here in details. For better understanding, the synthesis details of different ANGO films (Table 1).

Table 1: Synthesis of ANGO films of different thickness with different amounts of GO.

Thickness (µm)	Concentration of aniline (M)	Amount of GO (g)		
		0.01	**0.05**	**0.1**
12	1	ANGO 1	ANGO 2	ANGO 3
6	0.4	ANGO 4	ANGO 5	ANGO 6
3	0.2	ANGO 7	ANGO 8	ANGO 9

The work was carried out at 298 K. In this work the same experiments were conducted at different temperatures-288 K, 308 K and 398 K.[24] Beyond this temperature range, LOD was found to be higher. Adsorption isotherms were constructed following the same procedure as reported in our previous work (not shown here), from which the corresponding $-\Delta G_{ad}$ values were evaluated.

RESULTS

Evaluation of different thermodynamic parameters

Reorganization energy

The Marcus diagram consists of two similar parabolas signifying the reactant and product energy surfaces as a function of the nuclear configuration coordinate.[25] The energy of the activated state can be expressed as,

$$\Delta G^{\#} = \frac{(\Delta G^0+\lambda)^2}{4\lambda} \ldots(1)^{25}$$

where, $\Delta G^{\#}$ denotes the free energy of activated state and the reaction barrier. In this work it is $-\Delta G_{ad}$. ΔG^0 is the Gibb's free energy difference of electron transfer at equilibrium, can be obtained using the following equation

$$\Delta G^0 = -nFE^0 \ldots(2)^{26}$$

Here, n is the number of electrons transferred, F is the Faraday's constant and E^0 is the standard electrode potential. The λ value can be evaluated from (1) and (2) using MATLAB. Since equation (1) is a quadratic equation, therefore two values of λ were achieved from which the minimum value was taken into consideration.

The λ value, can be used to calculate the solvated ionic radius of Cd^{2+} as a measure of the sensor performance due to change in with film thickness or amount of GO using the equation (3).

$$\lambda = e^2\left(\frac{1}{\epsilon_0}-\frac{1}{\epsilon_S}\right)\left(\frac{1}{2a}+\frac{1}{2b}-\frac{1}{d}\right)\ldots(3)^{12}$$

Here, e is the charge transferred, ε_S is the dielectric constant of solvent (here dielectric coefficient of water was taken into consideration since the concentration of Cd^{2+} is very low), ε_0 is the relative permittivity of the vacuum, a is assumed to be the thickness (1 nm) of SAM where Cd^{2+} ions gets adsorbed, b is the solvated ionic radius of Cd^{2+} and d is considered as the BW values as evaluated in our previous work.[4]

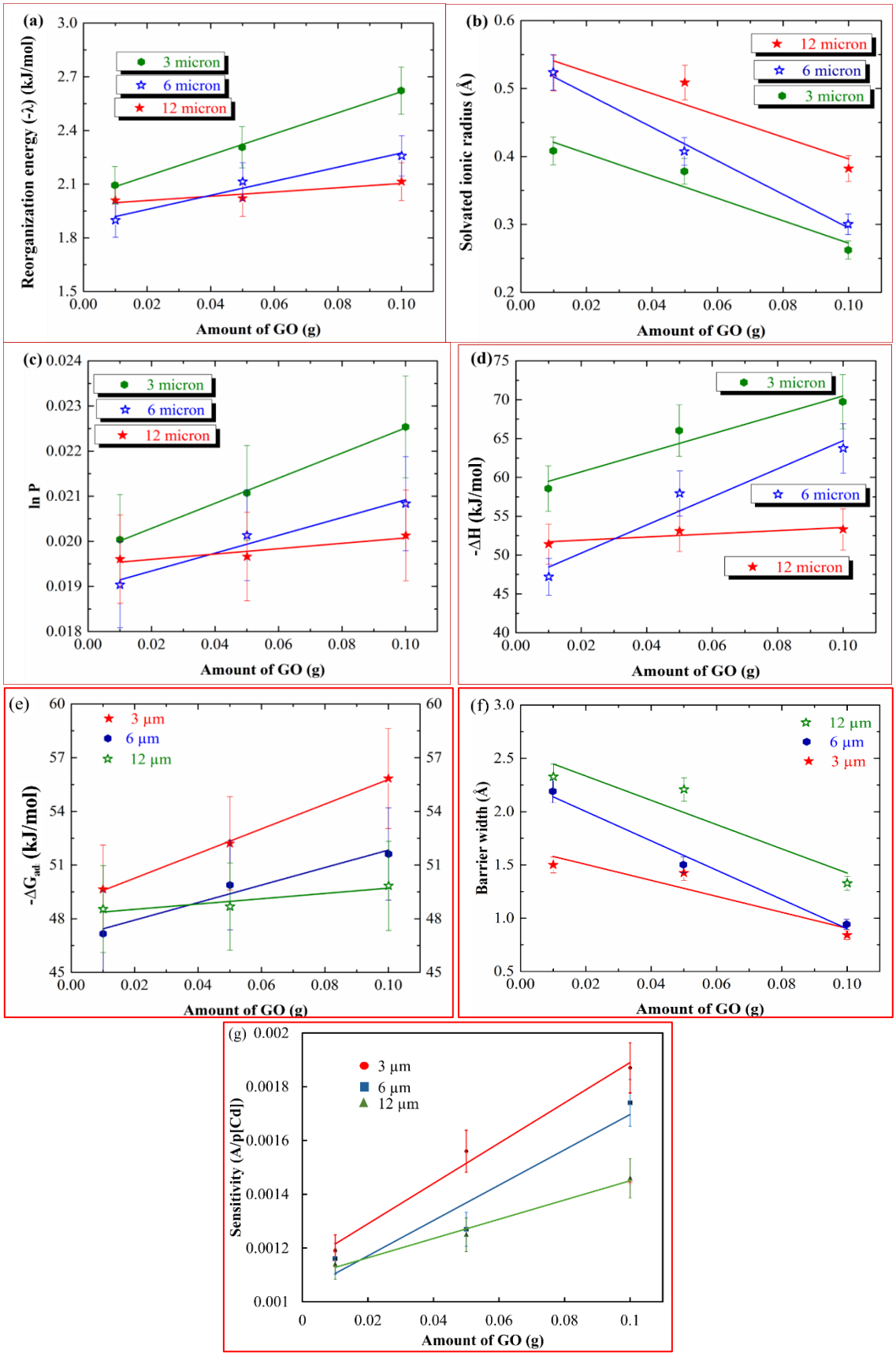

Figure 2 (A-G): Variation of reorganization energy, solvated ionic radius, in P and -ΔH, -ΔG_{ad}, d and sensitivity against amount of GO for each film thicknesses.

The reorganization energy values (-λ) and solvated ionic radii were plotted against amount of GO at different film thicknesses and shown in Figure 2 A and B respectively and the corresponding slopes (S_λ) and (S_{SR}) were evaluated and listed in Table 2.

Partition coefficient

Equation (4) was used to evaluate partition coefficient (ln P)

$$\Delta G = -RT \ln P \quad \ldots(4)^{27}$$

ΔG is the Gibb's free energy, R and T are the universal gas constant and temperature respectively.

The partition coefficient P also can be expressed by Van't Hoff equation

$$\Delta G = 2.303 \log P \ldots(5)^{27}$$

Where, ΔG, the Gibb's free energy can be correlated to enthalpy and entropy by the following expression.

$$\Delta G = \Delta H - T\Delta S \quad \ldots(6)$$

where ΔH, ΔS and T are the enthalpy, entropy and temperature respectively. It can be estimated that for two separate cases with two closer values of log P, there is a possibility of large difference in enthalpy or entropy indicating different partitioning mechanisms signifying the difference in charge distribution in electrode surface to the electrolyte.

The ln P values were plotted against the amount of GO content for each film thicknesses, shown in Figure 2 C. The slopes (S_{PC}) were evaluated and listed in Table 2.

Enthalpy

To calculate the ΔH values, Van't Hoff's isochore can be used as shown in equation (4)

$$\Delta G = 2.303 \frac{\Delta H}{RT} + Constant \ldots(7)$$

This method is based on the assumption that the ion partitioning is constant over the range of temperature.[21]

To calculate the enthalpy value, the values of $-\Delta G_{ad}$ obtained at different temperatures were put into equation (5) to evaluate log P. Further, the plots of (1000/T) vs log P for Cd^{2+} for varying amount of GO in ANGO at different film thicknesses were constructed and slopes were evaluated. From the equation (6), ΔH values were calculated using the slopes. Figure 2 D shows plots of -ΔH with respect to amount of GO at different film thicknesses and the corresponding slopes ($S_{\Delta H}$) are listed in Table 2.

Table 2: Slopes S_λ, S_{SR}, S_{PC}, $S_{\Delta H}$, S_G and S_d obtained from Figure 2.

Film thickness	S_λ (kJ/mol g)	S_{SR} (Å/g)	S_{PC}	$S_{\Delta H}$ (kJ/mol g)	S_G (kJ/mol g)	-S_d (Å/ g)	S_S (A/p[Cd])
12 µm	1.191	1.603	0.00595	20.602	68.97	8.6	0.0036
6 µm	3.951	2.471	0.01995	188.119	48.93	12.22	0.0066
3 µm	5.898	1.652	0.02784	122.013	14.81	12.32	0.0075

Table 3: Correlation coefficients relating various thermodynamic parameters, charge transport parameters and sensitivity.

Correlation factors	Correlations	Unit	Values and remarks
Sensitivity, reorganization energy and BW	$a_1 = \frac{S_S(\log(-S_d))}{S_\lambda}$	[A Å mol kJ $^{-1}$ g^{-1} (p[Cd])$^{-1}$]	The value of a_1 was almost constant and lies in the range 0.0014-0.0028. For lower film thickness, a_1 decreases.
Sensitivity with BW and partition coefficient,	$a_2 = \frac{S_S(\log(-S_d))}{(S_{PC})}$	[A Å g^{-1} (p[Cd])$^{-1}$]	The value of a_2 was almost constant (0.29-0.57). To get better response from sensor, the correlation coefficient value should be ~0.6.
Sensitivity, BW and enthalpy	$a_3 = \frac{S_S(\log(-S_d))}{(logS_{\Delta H})}$	A Å mol kJ $^{-1}$ g^{-1} (p[Cd])$^{-1}$]	The value of a_3 was almost constant and lies in the range 0.0025-0.004.
Solvated ionic radius and BW	$a_4 = \frac{S_{SR}}{(-S_d)}$	--	The value of a_4 is almost constant and lies within the range 0.013-0.020.
Enthalpy and BW	$a_5 = \frac{\log S_{\Delta H}}{(-S_d)}$	kJ mol^{-1}Å^{-1}	The value of $a_5$is almost constant and lies between 0.15-0.18

Evaluation of thermodynamic parameters for polyaniline based different sensing materials with different electrochemical surface area

Relation between enthalpy, ion partitioning, and reorganisation energy with electroactive surface area (A_S) obtained with different sensing materials-PA (polyaniline film), AN (copolymer of aniline and N-phenylglycine), AGO (composite from aniline and GO) and ANGO 3. Electrode film thickness for all films were 12 µm. A_S, LOD for Cd^{2+} detection and $-\Delta G_{ad}$ values (Table 4).

From $-\Delta G_{ad}$ values, (-λ) values were evaluated using equation (1) and (2); ln P values were calculated using equation (4). From the P values, ΔH values were for all the films using equation (6). Log P values were plotted against (1000/T) and from the slopes ΔH values were evaluated. Higher the electrochemical surface area (ESA) (A_S), higher was the diffusion across the double layer and adsorption of ions across the active sites which improved the sensor performance.

The increase in -ΔH was complementary to the analysis. Similar trend was observed in case of ln P and λ.

Table 4: Comparison of different films.

Film	Electro-active surface area (ESA) (cm^2)[4]	LOD for Cd^{2+} detection by SWV[4]	$-\Delta G_{ad}$ (kJ/mol)
PA	0.297	10 ppm	38.74
AN	0.458	50 ppb	49.53[24]
AGO	0.351	80 ppb	48.67
ANGO 3	0.566	25 ppb	49.864[4]

Table 5: Different correlation obtained between A_S and thermodynamic and charge transport parameters for different sensing materials.

Factors	Correlations	PA	AN	AGO	ANGO 3
A_S and (-λ)	$b_1 = A_S/(-\lambda)$, unit –cm^2 mol/kJ	0.228	0.219	0.174	0.268
A_S and ln P	$b_2 = A_S/\ln P$, unit – cm^2	0.019	0.023	0.018	0.028
A_S and (-ΔH)	$b_3 = A_S/(-\Delta H)$, unit –cm^2 mol/kJ	0.0071	0.0088	0.0074	0.0114
A_S and ($-\Delta G_{ad}$)	$b_1 = A_S/(-\Delta G)$, unit –cm^2 mol/kJ	0.0077	0.0092	0.0075	0.0112

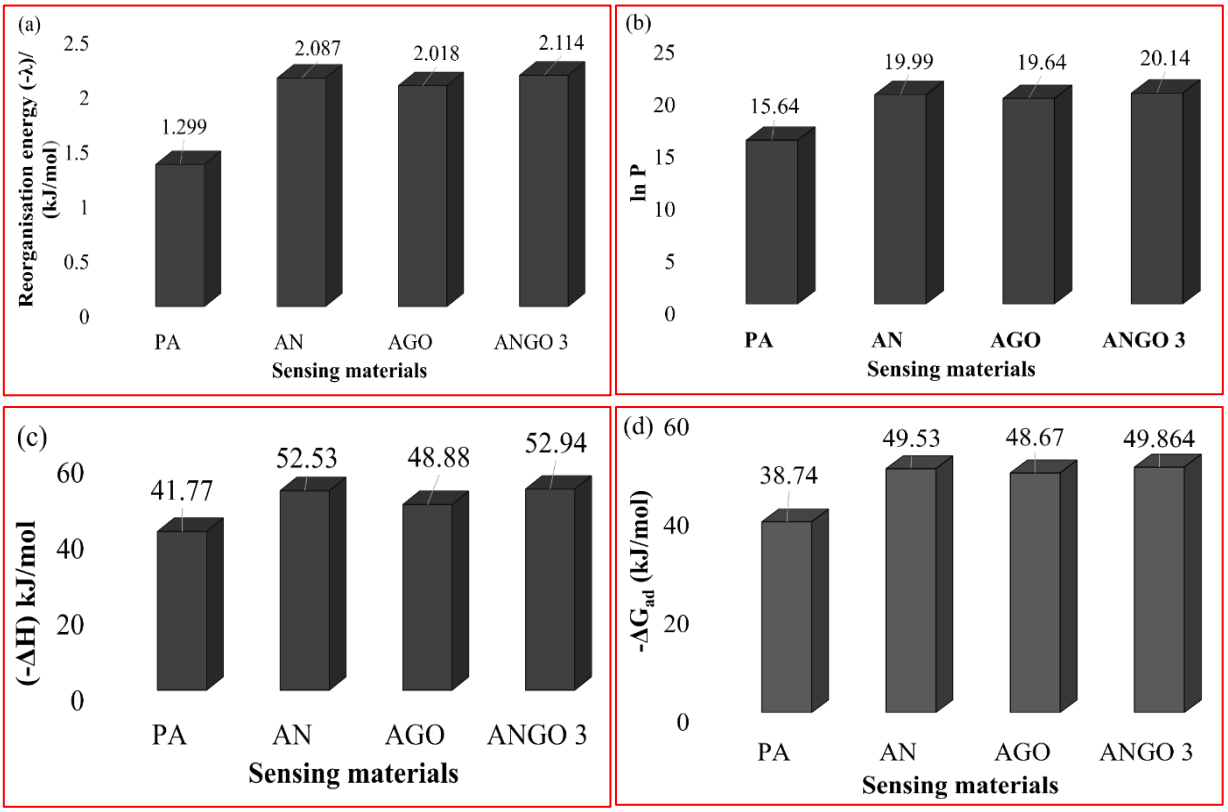

Figure 3 (A-D): Variation of (-λ), ln P, (-ΔH) and ($-\Delta G_{ad}$) for different films-PA, AN, AGO and ANGO 3.

DISCUSSION

Evaluation of different thermodynamic parameters

Reorganization energy

From Figure 2 A it can be observed that, the reorganization energy (-λ) for Cd^{2+} at film thickness of 12 µm was lowest at each amount of GO as compared to 6 and 3 µm and was higher for 3 µm. The slope S_λ for 12 µm thickness was the lowest as compared to other film indicating that increase in amount of GO does not bring significant effect for higher film thickness. From the definition of reorganization energy, as mentioned earlier, it indicates the energy required to distort the nuclear configuration from the reactant to the product states, therefore, it can be understood that higher reorganization energy value for lower film thickness indicates higher interaction at equilibrium.

Figure 2 B showed the variation of solvated ionic radius against the different amount of GO at different film thicknesses. The Cd^{2+} concentration was taken to be 10 ppb. The BW values for 10 ppb of Cd^{2+} at different film thicknesses and amount of GO were mentioned in our previous work.[4] Mobasherpour et al had reported that the solvated ionic radius for Cd^{2+} was 4.26 Å.[28] The concentration of Cd^{2+} was very high as compared to 100 ppb of Cd^{2+}. Othman et al have reported the hydrated ionic radius for Cd^{2+} was 2.63 Å.[29] Chen et al have reported 4.26 Å to be the hydrates ionic radius for Cd^{2+}.[30] In all the cases the concentration of Cd^{2+} was higher than 10 ppb-in molar level. In most cases different procedures for evaluation of solvated ionic radius were opted. Therefore, the ionic radius can be different. As reported in literature, the crystal ionic radius, Stokes and hydrated ionic radius for Cd^{2+} was 0.97, 3.41 and 2.63 Å.[31] In several works, the authors have considered the above reported value for their works. To the best of our knowledge, the solvated ionic radius for Cd^{2+} was not calculated by any other researchers using the Marcus theory of electron transfer incorporating BW based on Simmon's model on electron tunneling.[5,12] The plots in Figure 2 B showed linear behavior and the slopes S_{SR} were evaluated and listed in Table 2. The solvated ionic radius was higher for film thickness of 12 µm as compared to 3 and 6 µm. It was decreasing with decrease in film thickness. It was found to be decreasing with amount of GO content. For efficient charge transport, the solvated ionic radius should be lower. Therefore, increase in film thickness and decrease in GO content increase the solvated ionic radius and hence lowers the charge transport.

Partition coefficient

From Figure 2 C, it can be observed that the partition coefficient values in case of 12 µm thicknesses were linear with a smaller slope of 0.00595 as compared to other films. It indicates the values of partition coefficient was not varying with significant differences which in turn can be understood that for higher thickness, increase in GO in ANGO does not bring much change in distribution of ions among the electrode electrolyte interface. For 12 µm thickness, the LOD was also higher as compared to 6 and 3 µm thicknesses. Highest values were observed with the film with thickness of 3 µm. From the plots the slopes S_{PC} were calculated and provided in Table 1.

Enthalpy

As observed from Figure 2 D, the -ΔH values show linear behavior with the amount of GO at each case and the slopes $S_{\Delta H}$ values were evaluated and provided in Table 2. In our earlier work, it was observed that for each of the films ANGO (1-9), the values were more than 40 kJ/mol.[4] At lower temperature in some cases the $-\Delta G_{ad}$ values were observed to be less than 40 kJ/mol. Generally, if the values were found to be more than 40 kJ/mol it indicates chemisorption.[32,33] Therefore, incorporation of GO in ANGO backbone increases the interaction between Cd^{2+} and the electrode surface. From Figure 2 D it is obvious that the enthalpy values also showed similar behavior as the ln P values. The slope for 12 µm thickness was the lowest as compared to the other films. Maximum value of enthalpy was observed for 3 µm thickness. As the thickness decreases the enthalpy value decreases. Similarly for each thickness with increase in GO increase in enthalpy was observed.

Correlation coefficients

The sensitivity values, $-\Delta G_{ad}$ and BW (d) values obtained from our earlier work for all the films were plotted against the amount of GO for each film thicknesses and corresponding slopes were evaluated. Amount of GO vs $-\Delta G_{ad}$ (Figure 2 E) delivered the slopes S_G, amount of GO vs d (Figure 2 F), delivered the slopes S_d and amount of GO vs sensitivity (Figure 2 G) delivered the slop S_S. Corresponding values of the slopes are mentioned in Table 2.

To relate thermodynamic parameters with sensitivity of the sensor and charge transport parameters, several simulations were carried out and a couple of correlations were achieved, listed in Table 3.

The advantage of these correlation coefficients is that by doing a small number of experiments, the entire thermodynamic properties and charge transport properties of the systems can be understood. To understand each properties, in general, series of experiments are required. Again, correlation coefficients help in designing different polyaniline based novel materials to detect Cd^{2+} at ultra low level, by performing handful number of experiments.

Relationship between electrochemical surface area and thermodynamic parameters

To find inter relation between the A_S and (-λ), ln P, (-ΔH) and $(-\Delta G_{ad})$, simple simulation was carried out by fitting all the parameters in different sets of equations and a set

of correlations were achieved which are listed in Table 5. The correlation coefficient of b_1 was achieved which was the ratio of As to (-λ) and lies in the range 0.23 to 0.27. Higher value of ln P was observed for the films with higher A_S as stated by correlation coefficient b_2 which is the ratio of A_S to ln P. The value of b_2 lies in the range ~0.19 to ~0.28. The increase in -ΔH value was observed for the films with higher ESA (A_S). The correlation coefficient b_3 is the ratio of A_S and (-ΔH) which lies in the range ~0.007 to ~0.01. The correlation coefficient b_3 is the ratio of A_S and ($-\Delta G_{ad}$) which lies in the range ~0.007 to ~0.01. All the correlation coefficient values were almost constant and lies in a smaller range. The utility of these correlation coefficient lies in the fact that how electrochemical surface area can influence the thermodynamic properties of the system and in order to build a novel polyaniline-based sensor for Cd^{2+} detection, these correlation coefficients should be taken into consideration.

Limitation

The films ANGO were not stable for longer period. It was observed that after 2 months upon storing in buffer of pH 3.3 at 4 °C, the films show degraded performance. For making the films commercially feasible it is important to work increasing the lifetime of the sensing films.

The correlation coefficients developed in this work are strictly restricted to polyaniline-based materials. In this ANGO system, aniline had the highest concentration in the electrolyte for synthesis of ANGO. Therefore, these correlation coefficients will be suitable for polyaniline based system. To check detailed thermodynamic and charge transport process for any other polymer-based system, similar experiments should be performed and new correlation coefficients should be developed.

CONCLUSION

This work is a follow up work of our previous works. In this work, the reorganization energy (-λ), solvated ionic radius, partition coefficient (ln P) and enthalpy (-ΔH) values for the ANGO (1-9) films with different amount of GO at different film thicknesses were evaluated. All the values were plotted against the amount of GO at different film thicknesses. The reorganization energy, enthalpy and partition coefficient were found to be increasing with increase in GO content and film thickness while the solvated ionic radius was decreasing with increase in GO content and film thickness favoring the charge transfer. Several correlation coefficients were achieved using thermodynamic, charge transport and detection parameters. The utility of these correlation coefficients lies in the fact that upon doing a small number of experiments, the entire thermodynamic properties of the systems can be understood which in general needs a series of experiments. Moreover, using such correlation coefficients polyaniline based novel materials can be designed to detect Cd^{2+} in any process streams or environmental pool or drinking water by performing a handful number of experiments.

A comparison based on A_S, -ΔH, ln P, (-λ) and ($-\Delta G_{ad}$) was conducted for different sensing films with different electroactive surface areas -PA, AN, AGO and ANGO 3. It was observed that PA has the lowest A_S, -ΔH, ln P, ($-\Delta G_{ad}$) and λ. As N-phenylglycine was incorporated into PA backbone, for AN films the sensing parameter values improved. For AGO film, improved performance was observed but AN was found to be better than AGO. Finally further improvement was observed by incorporation of N-phenylglycine and GO into PA which delivered highest A_S, -ΔH, ln P, ($-\Delta G_{ad}$) and λ. Various correlation coefficients were achieved indicating relation between As with -ΔH, ln P and λ, ln P, -ΔH and ($-\Delta G_{ad}$) as listed in Table 3. These correlation coefficients gives a clear idea how thermodynamic properties of a sensor can be influenced by electrochemical surface area and they should be taken into consideration while developing a novel polyaniline based Cd^{2+} sensor.

Funding: Funding sources by Ministry of Electronics and Information Technology, Government of India (grant number 2(4)/2014-PEGD (IPIIW)).
Conflict of interest: None declared
Ethical approval: The study was approved by the Institutional Ethics Committee

REFERENCES

1. Adhawiyah RE, Lee J. Enhancing Sensitivity and Selectivity: Morphological Modification and Chemical Functionalization within Confined Structures. Int J Precision Engineering Manufacturing. 2024;25(4):875-95.
2. Gao F, Chunxiu L, Lichao Z, Tiezhu L, Zheng W, Zixuan S, et al. Wearable and flexible electrochemical sensors for sweat analysis: a review. Microsyst Nanoeng. 2023;9(1):1-21.
3. Montmeat P, Pijolat C, Tournier G, Viricelle JP. The influence of a platinum membrane on the sensing properties of a tin dioxide thin film. Sens Actuators B Chem. 2002;84(2):148-59.
4. Dutta K, Panda S. Thermodynamic and Charge Transport Studies for the Detection of Heavy Metal Ions in Electrochemical Sensors Using a Composite Film of Aniline, N-phenylglycine and Graphene Oxide. J Electrochem Soc. 2019;166(14):B13355.
5. Vilan A. Analyzing Molecular Current-Voltage Characteristics with the Simmons Tunneling Model: Scaling and Linearization. J Physical Chemistry C. 2007;111(11):4431-44.
6. Akkerman HB, Naber RCG, Jongbloed B, Van Hal PA, Blom PWM, De Leeuw DM, et al. Electron tunneling through alkanedithiol self-assembled monolayers in large-area molecular junctions. Proceedings National Academy Sci. 2007;104(27):11161-6.

7. Hill CM, Kim J, Bard AJ. Electrochemistry at a Metal Nanoparticle on a Tunneling Film: A Steady-State Model of Current Densities at a Tunneling Ultramicroelectrode. J Am Chem Soc. 2015;137(35):11321-6.
8. Hill CM, Kim J, Bodappa N, Bard AJ. Electrochemical Nonadiabatic Electron Transfer via Tunneling to Solution Species through Thin Insulating Films. J Am Chem Soc. 2017;139(17):6114-9.
9. Solak AO, Eichorst LR, Clark WJ, McCreery RL. Modified Carbon Surfaces as 'Organic Electrodes' That Exhibit Conductance Switching. Anal Chem. 2003;75(2):296-305.
10. Tseng SH, Peng-Chung JJ, Chuan-Mei T, Tsai-Mu C, Hsueh-Liang C, Yu-Chuan C, et al. Ni2+-Enhanced Charge Transport via π-π Stacking Corridor in Metallic DNA Biophys J. 2011;100(4):1042-48.
11. Khoshroo M, Rostami AA, Yeganegi S. Cyclic voltammetric and computational study of a 4-bromophenyl monolayer on a glassy carbon electrode. Monatshefte für Chemie-Chemical Monthly. 2008;139(7):781-7.
12. Sharp KA. Calculation of electron transfer reorganization energies using the finite difference Poisson-Boltzmann model. Biophys J. 1998;74(3):1241-50.
13. Eckermann AL, Feld DJ, Shaw DJ, Meade TJ. Electrochemistry of redox-active self-assembled monolayers. Coord Chem Rev. 2010;254(15-16):1769-802.
14. Marcus RA. Tight-binding approximation for semi-infinite solids. Application of a transform method and of delta function normalization. J Chem Phys. 1993;98(7):5604-11.
15. Gosavi S, Marcus RA. Nonadiabatic Electron Transfer at Metal Surfaces. J Phys Chem B. 2000;104(9):2067-72.
16. Miller NE, Wander MC, Cave RJ. A Theoretical Study of the Electronic Coupling Element for Electron Transfer in Water. J Phys Chem A. 1999;103(8):1084-93.
17. Cave RJ, Newton MD. Calculation of electronic coupling matrix elements for ground and excited state electron transfer reactions: Comparison of the generalized Mulliken–Hush and block diagonalization methods. J Chem Phys. 1997;106(22):9213-26.
18. Marcus RA. Chemical and Electrochemical Electron-Transfer Theory. Annu Rev Phys Chem. 1964;15(1):155-96.
19. Newton MD, Sutin N. Electron Transfer Reactions in Condensed Phases. Annu Rev Phys Chem. 1984;35(1):437-80.
20. Johanson G. Modeling of Disposition. Comprehensive Toxicol. 2010;153-77.
21. Dearden J, Bresnen G. Thermodynamics of Water-octanol and Water-cyclohexane Partitioning of some Aromatic Compounds. Int J Mol Sci. 2005;6(1):119-29.
22. Papamichael EM, Stamatis H, Stergiou PY, Foukis A, Gkini OA. Enzyme Kinetics and Modeling of Enzymatic Systems. Adv Enzyme Technol. 2019;71-104.
23. Dutta K, Panda S. Estimation of thermodynamics properties as a measure of the extent of interference in a conducting polymer based electrochemical aqueous ion sensor. Int J Scientific Rep. 2024;10(4):102-10.
24. Dutta K, Panda S. Identification of the Levels of Interference of Ions toward Heavy Metal Detection in Electrochemical Sensors Using the Barrier Width Technique. J Electrochem Soc. 2018;165(9):B378.
25. Houchins G, Pande V, Viswanathan V. Mechanism for Singlet Oxygen Production in Li-Ion and Metal-Air Batteries. ACS Energy Lett. 2020;5(6):1893-9.
26. Bard AJ, Faulkner LR, White HS. Electrochemical methods: fundamentals and applications, 2nd ed. John Wiley and Sons. 2022.
27. Dutra LMU, Ribeiro MENP. Binary mixture micellar systems of F127 and P123 for griseofulvin solubilization. Polímeros. 2015;25(5):433-9.
28. Mobasherpour I, Salahi E, Pazouki M. Comparative of the removal of Pb2+, Cd2+ and Ni2+ by nano crystallite hydroxyapatite from aqueous solutions: Adsorption isotherm study. Arab J Chem. 2012;5(4):439-46.
29. Al Hamouz OCS, Ali SA. Removal of Zinc and Cadmium Ions Using a Cross-linked Polyaminophosphonate. J Macromolecular Sci Part A. 2013;50(4):375-84.
30. Chen SB, Ma YB, Chen L, Xian K. Adsorption of aqueous Cd2+, Pb2+, Cu2+ ions by nano-hydroxyapatite: Single- and multi-metal competitive adsorption study. Geochem J. 2010;44(3):233-9.
31. Nightingale ER. Phenomenological Theory of Ion Solvation. Effective Radii of Hydrated Ions. J Phys Chem. 1959;63(9):1381-7.
32. Jnr MH, Spiff AI, Abia A. Studies on the Influence of Mercaptoacetic Acid (MAA) Modification of Cassava (Manihot sculenta Cranz) Waste Biomass on the Adsorption of Cu 2+ and Cd 2+ from Aqueous Solution. Bull Korean Chem Soc. 2004;25(7):969-76.
33. Kumar PS, Ramakrishnan K, Kirupha SD, Sivanesan S. Thermodynamic and kinetic studies of cadmium adsorption from aqueous solution onto rice husk. Brazilian J Chem Engineering. 2010;27(2):347-55.

Cite this article as: Dutta K, Panda S. Explanation based on thermodynamic parameters regarding effect of sensing film thickness and amount of graphene oxide on sensor performance in aniline, N-phenylglycine and graphene oxide based electrochemical heavy metal ion sensor. Int J Sci Rep 2024;10(7):225-33.